

Effect of the N3LO three-nucleon contact interaction on $p - d$ scattering observables

L. Girlanda^{1,2}, E. Filandri^{1,2}, A. Kievsky³, L.E. Marcucci^{3,4} and M. Viviani³

¹*Department of Mathematics and Physics “E. De Giorgi”,*

University of Salento, I-73100 Lecce, Italy

²*INFN-Lecce, I-73100 Lecce, Italy*

³*INFN-Pisa, I-56127, Pisa, Italy*

⁴*Department of Physics “E. Fermi”,*

University of Pisa, I-56127 Pisa, Italy

(Dated: February 8, 2023)

A unitary transformation allows to remove redundant terms in the two-nucleon (2N) contact interaction at the fourth order (N3LO) in the low-energy expansion of Chiral Effective Field Theory. In so doing a three-nucleon (3N) interaction is generated. We express its short-range component in terms of five combinations of low-energy constants (LECs) parametrizing the N3LO 2N contact Lagrangian. Within a hybrid approach, in which this interaction is considered in conjunction with the phenomenological AV18 2N potential, we show that the involved LECs can be used to fit very accurate data on polarization observables of low-energy $p - d$ scattering, in particular the A_y asymmetry. The resulting interaction is of the right order of magnitude for a N3LO contribution.

I. INTRODUCTION

The effective field theory (EFT) framework is nowadays the standard setting to address the nuclear interaction problem. Starting from the choice of low-energy active degrees of freedom, it allows to express physical observables in terms of low-energy constants (LECs) in a systematic expansion in powers of a small parameter representing the separation of scales [1–4]. All the short-distance effects from the frozen degrees of freedom are effectively encoded in the values of the LECs, which parametrize contact interactions. Being unconstrained by the imposed symmetries, the LECs have to be fitted from experimental data, at the cost of the predictive power of the EFT. From another perspective, they may provide the needed flexibility to accurately model the nuclear interaction. For example, Chiral EFT (ChEFT) makes use of the approximate chiral symmetry of strong interaction to severely constrain the interaction of pions and nucleons. According to the common wisdom, in the isospin limit there are two LECs contributing at the leading order (LO) in the two-nucleon (2N) sector, traditionally called C_S and C_T , seven ($C_{i=1,\dots,7}$) at the next-to-leading order (NLO), and fifteen more ($D_{i=1,\dots,15}$) at the next-to-next-to-next-to leading order (N3LO). The three-nucleon (3N) sector is much more constrained. The first contributions arise at the next-to-next-to leading order (N2LO) [5, 6], parametrized by two LECs, C_D and C_E , the former of which is actually a weak two-nucleon LEC, contributing for example to the muon capture from deuterium [7–10]. At the fifth order (N4LO) we find the contribution of thirteen more LECs, $E_{i=1,\dots,13}$ [11]. However, the distinction between 2N and 3N LECs is, to some extent, a matter of convention, depending on the arbitrary choice for the nucleon interpolating field: non-linear field redefinitions may change a seemingly 2N interaction into a 3N one, without changing the predictions for the on-shell quantities. Thus, it was observed in Ref. [12] that three out of the fifteen 2N independent con-

tact interactions arising at N3LO can be made to vanish by a suitable unitary transformation, inducing specific modifications of the 3N interaction. In Ref. [13] we exhibited the precise form of the induced 3N interaction. Moreover, we identified two additional 2N contact LECs at N3LO parametrizing momentum dependent interactions allowed by Poincaré symmetry, which we named D_{16} and D_{17} . They can also be transformed, through a unitary transformation, into a 3N interaction. Thus, contrary to widespread belief [16, 17], five adjustable LECs parametrize the 3N interaction at N3LO of the chiral expansion. This could be the explanation of all failed attempts to improve the accuracy in 3N systems (particularly for scattering observables) when going from N2LO to N3LO [18]. On the other hand, the inclusion of the N4LO 3N contact interaction has already proved to be of great importance in reducing existing discrepancies between theory and experimental data [19, 20]. In the present paper we provide quantitative evidence that the five extra LECs at N3LO ensure sufficient flexibility to drastically improve the description of low-energy $p - d$ scattering polarization observables, most notably the A_y asymmetry, which constitutes a long-standing problem for most nuclear interaction models. We do this in a hybrid approach in which the induced 3N force (restricted to its shortest range part) is considered in conjunction with the phenomenological AV18 2N potential [21], deferring a consistent calculation in ChEFT to future work. The paper is organized as follows. In Section II we start from the N3LO 2N Hamiltonian comprising 17 independent LECs and identify the unitary transformation allowing to restrict oneself to a subset of twelve independent LECs. In Section III the corresponding induced 3N contact interaction are worked out and written in the minimal basis of thirteen independent subleading operators of Ref. [11]. Despite being formally of N4LO, these specific terms are promoted in the chiral counting to N3LO, due to the enhancement produced by the dependence on the large nucleon mass. In Section IV we briefly describe

the calculation of low-energy $p-d$ scattering observables below the breakup threshold based on the Hyperspherical Harmonics (HH) method [22, 23]. In Section V we fit the 5 N3LO LECs to very precise data on polarized $p-d$ scattering at 2 MeV center-of-mass energy [24] using the induced 3N interaction on the top of the AV18 2N phenomenological potential. Finally, we summarize our findings and outline directions for future developments in the conclusions of Section VI.

II. N3LO 2N CONTACT HAMILTONIAN

The N3LO 2N contact potential was originally considered in Refs. [25, 26] as consisting of 15 LECs. After careful scrutiny of the constraints imposed by Poincaré symmetry, two further LECs emerge [13], leading to the following expression in the general reference frame,

$$\begin{aligned}
V_{NN}^{(4)} = & D_1 k^4 + D_2 Q^4 + D_3 k^2 Q^2 + D_4 (\mathbf{k} \times \mathbf{Q})^2 + [D_5 k^4 \\
& + D_6 Q^4 + D_7 k^2 Q^2 + D_8 (\mathbf{k} \times \mathbf{Q})^2] (\boldsymbol{\sigma}_1 \cdot \boldsymbol{\sigma}_2) \\
& + \frac{i}{2} (D_9 k^2 + D_{10} Q^2) (\boldsymbol{\sigma}_1 + \boldsymbol{\sigma}_2) \cdot (\mathbf{Q} \times \mathbf{k}) \\
& + (D_{11} k^2 + D_{12} Q^2) (\boldsymbol{\sigma}_1 \cdot \mathbf{k}) (\boldsymbol{\sigma}_2 \cdot \mathbf{k}) \\
& + (D_{13} k^2 + D_{14} Q^2) (\boldsymbol{\sigma}_1 \cdot \mathbf{Q}) (\boldsymbol{\sigma}_2 \cdot \mathbf{Q}) \\
& + D_{15} \boldsymbol{\sigma}_1 \cdot (\mathbf{k} \times \mathbf{Q}) \boldsymbol{\sigma}_2 \cdot (\mathbf{k} \times \mathbf{Q}) \\
& + i D_{16} \mathbf{k} \cdot \mathbf{Q} \mathbf{Q} \times \mathbf{P} \cdot (\boldsymbol{\sigma}_1 - \boldsymbol{\sigma}_2) \\
& + D_{17} \mathbf{k} \cdot \mathbf{Q} (\mathbf{k} \times \mathbf{P}) \cdot (\boldsymbol{\sigma}_1 \times \boldsymbol{\sigma}_2)
\end{aligned} \quad (1)$$

with $\mathbf{k} = \mathbf{p}' - \mathbf{p}$ and $\mathbf{Q} = \frac{\mathbf{p}' + \mathbf{p}}{2}$, \mathbf{p} and \mathbf{p}' being the initial and final relative momenta, and $\mathbf{P} = \mathbf{p}_1 + \mathbf{p}_2$ the total pair momentum. However, as it was pointed out in Ref. [12], only 12 independent LECs survive on shell and can thus be determined from 2N scattering data. This redundancy amounts to a unitary ambiguity, i.e. to the possibility of generating shifts of the LECs by unitary transforming the one-body kinetic energy operator H_0 as

$$H_0 \rightarrow U^\dagger H_0 U, \quad (2)$$

where U is the most general unitary 2-body contact transformation depending on 5 arbitrary parameters α_i ,

$$U = \exp \left[\sum_{i=1}^5 \alpha_i T_i \right], \quad (3)$$

and the independent generators T_i were given explicitly in Ref. [13] as

$$T_1 = \int d^3 \mathbf{x} N^\dagger \overleftrightarrow{\nabla}^i N \nabla^i (N^\dagger N), \quad (4)$$

$$T_2 = \int d^3 \mathbf{x} N^\dagger \overleftrightarrow{\nabla}^i \sigma^j N \nabla^i (N^\dagger \sigma^j N), \quad (5)$$

$$\begin{aligned}
T_3 = \int d^3 \mathbf{x} \left[N^\dagger \overleftrightarrow{\nabla}^i \sigma^i N \nabla^j (N^\dagger \sigma^j N) \right. \\
\left. + N^\dagger \overleftrightarrow{\nabla}^i \sigma^j N \nabla^j (N^\dagger \sigma^i N) \right], \quad (6)
\end{aligned}$$

$$T_4 = i \epsilon^{ijk} \int d^3 \mathbf{x} N^\dagger \overleftrightarrow{\nabla}^i N N^\dagger \overleftrightarrow{\nabla}^j \sigma^k N, \quad (7)$$

$$\begin{aligned}
T_5 = \int d^3 \mathbf{x} \left[N^\dagger \overleftrightarrow{\nabla}^i \sigma^i N \nabla^j (N^\dagger \sigma^j N) \right. \\
\left. - N^\dagger \overleftrightarrow{\nabla}^i \sigma^j N \nabla^j (N^\dagger \sigma^i N) \right], \quad (8)
\end{aligned}$$

with $N^\dagger \overleftrightarrow{\nabla}^i N = N^\dagger (\nabla^i N) - (\nabla^i N^\dagger) N$, and $N(x)$ denoting the non-relativistic nucleon field operators.

The transformation (3) entails a shift of the N3LO contact LECs, $D_i \rightarrow D_i + \delta D_i$, with

$$\delta D_3 = -\frac{4}{m} \alpha_1, \quad (9)$$

$$\delta D_4 = \frac{4}{m} \alpha_1, \quad (10)$$

$$\delta D_7 = -\frac{4}{m} \alpha_2, \quad (11)$$

$$\delta D_8 = \frac{4}{m} \alpha_2 + \frac{2}{m} \alpha_3, \quad (12)$$

$$\delta D_{15} = -\frac{4}{m} \alpha_3, \quad (13)$$

$$\delta D_{12} = -\frac{4}{m} \alpha_3, \quad (14)$$

$$\delta D_{13} = -\frac{4}{m} \alpha_3, \quad (15)$$

$$\delta D_{16} = -\frac{2}{m} \alpha_4, \quad (16)$$

$$\delta D_{17} = -\frac{4}{m} \alpha_3 - \frac{2}{m} \alpha_5, \quad (17)$$

and the remaining ones being zero. Here m is the nucleon mass. By choosing

$$\alpha_1 = \frac{m}{16} (16D_1 + D_2 + 4D_3), \quad (18)$$

$$\alpha_2 = \frac{m}{16} (16D_5 + D_6 + 4D_7), \quad (19)$$

$$\alpha_3 = \frac{m}{32} (D_{14} + 16D_{11} + 4D_{12} + 4D_{13}), \quad (20)$$

$$\alpha_4 = \frac{m}{2} D_{16}, \quad (21)$$

$$\alpha_5 = \frac{m}{16} (8D_{17} - D_{14} - 16D_{11} - 4D_{12} - 4D_{13}), \quad (22)$$

the N3LO contact potential is brought in the form of

Ref. [12],

$$\begin{aligned}
V_{NN}^{(4)} = & D'_1 [k^4 - 4(\mathbf{Q} \cdot \mathbf{k})^2] + D'_2 \left[Q^4 - \frac{1}{4}(\mathbf{Q} \cdot \mathbf{k})^2 \right] \\
& + D'_3 (\mathbf{k} \times \mathbf{Q})^2 \\
& + \left\{ D'_4 [k^4 - 4(\mathbf{Q} \cdot \mathbf{k})^2] + D'_5 \left[Q^4 - \frac{1}{4}(\mathbf{Q} \cdot \mathbf{k})^2 \right] \right. \\
& \left. + D'_6 (\mathbf{k} \times \mathbf{Q})^2 \right\} \boldsymbol{\sigma}_1 \cdot \boldsymbol{\sigma}_2 \\
& + \frac{i}{2} (D'_7 k^2 + D'_8 Q^2) (\boldsymbol{\sigma}_1 + \boldsymbol{\sigma}_2) \cdot (\mathbf{Q} \times \mathbf{k}) \\
& + D'_9 \left(-\frac{1}{4} k^2 \boldsymbol{\sigma}_1 \cdot \mathbf{k} \boldsymbol{\sigma}_2 \cdot \mathbf{k} + 4Q^2 \boldsymbol{\sigma}_1 \cdot \mathbf{Q} \boldsymbol{\sigma}_2 \cdot \mathbf{Q} \right) \\
& + D'_{10} Q^2 (\boldsymbol{\sigma}_1 \cdot \mathbf{k} \boldsymbol{\sigma}_2 \cdot \mathbf{k} - 4\boldsymbol{\sigma}_1 \cdot \mathbf{Q} \boldsymbol{\sigma}_2 \cdot \mathbf{Q}) \\
& + D'_{11} (k^2 - 4Q^2) \boldsymbol{\sigma}_1 \cdot \mathbf{Q} \boldsymbol{\sigma}_2 \cdot \mathbf{Q} \\
& + D'_{12} \boldsymbol{\sigma}_1 \cdot (\mathbf{k} \times \mathbf{Q}) \boldsymbol{\sigma}_2 \cdot (\mathbf{k} \times \mathbf{Q}), \tag{23}
\end{aligned}$$

with the following identifications

$$D'_1 = D_1, \tag{24}$$

$$D'_2 = D_2, \tag{25}$$

$$D'_3 = D_3 + D_4, \tag{26}$$

$$D'_4 = D_5, \tag{27}$$

$$D'_5 = D_6, \tag{28}$$

$$D'_6 = D_7 + D_8 + \frac{1}{16} D_{14} + D_{11} + \frac{1}{4} D_{12} + \frac{1}{4} D_{13}, \tag{29}$$

$$D'_7 = D_9, \tag{30}$$

$$D'_8 = D_{10}, \tag{31}$$

$$D'_9 = -4D_{11}, \tag{32}$$

$$D'_{10} = -\frac{1}{8} D_{14} - 2D_{11} + \frac{1}{2} D_{12} - \frac{1}{2} D_{13}, \tag{33}$$

$$D'_{11} = -\frac{1}{8} D_{14} - 2D_{11} - \frac{1}{2} D_{12} + \frac{1}{2} D_{13}, \tag{34}$$

$$D'_{12} = D_{15} - 2D_{11} - \frac{1}{2} D_{12} - \frac{1}{2} D_{13} - \frac{1}{8} D_{14}. \tag{35}$$

III. INDUCED 3N CONTACT INTERACTIONS

When applied to the LO 2N contact Hamiltonian,

$$V_{NN}^{(0)} = C_S + C_T \boldsymbol{\sigma}_1 \cdot \boldsymbol{\sigma}_2, \tag{36}$$

the unitary transformation (3) induces additional 3N interactions [13] which can be viewed as a modification of the subleading 3N contact interaction entering at N4LO

of the low-energy expansion [11],

$$\begin{aligned}
V_{3N}^{(2)} = & \sum_{ijk} \left(-E_1 \mathbf{k}_i^2 - E_2 \mathbf{k}_i^2 \boldsymbol{\tau}_i \cdot \boldsymbol{\tau}_j \right. \\
& - E_3 \mathbf{k}_i^2 \boldsymbol{\sigma}_i \cdot \boldsymbol{\sigma}_j - E_4 \mathbf{k}_i^2 \boldsymbol{\sigma}_i \cdot \boldsymbol{\sigma}_j \boldsymbol{\tau}_i \cdot \boldsymbol{\tau}_j \\
& - E_5 (3\mathbf{k}_i \cdot \boldsymbol{\sigma}_i \mathbf{k}_i \cdot \boldsymbol{\sigma}_j - \mathbf{k}_i^2 \boldsymbol{\sigma}_i \cdot \boldsymbol{\sigma}_j) \\
& - E_6 (3\mathbf{k}_i \cdot \boldsymbol{\sigma}_i \mathbf{k}_i \cdot \boldsymbol{\sigma}_j - \mathbf{k}_i^2 \boldsymbol{\sigma}_i \cdot \boldsymbol{\sigma}_j) \boldsymbol{\tau}_i \cdot \boldsymbol{\tau}_j \\
& + \frac{i}{2} E_7 \mathbf{k}_i \times (\mathbf{Q}_i - \mathbf{Q}_j) \cdot (\boldsymbol{\sigma}_i + \boldsymbol{\sigma}_j) \\
& + \frac{i}{2} E_8 \mathbf{k}_i \times (\mathbf{Q}_i - \mathbf{Q}_j) \cdot (\boldsymbol{\sigma}_i + \boldsymbol{\sigma}_j) \boldsymbol{\tau}_j \cdot \boldsymbol{\tau}_k \\
& - E_9 \mathbf{k}_i \cdot \boldsymbol{\sigma}_i \mathbf{k}_j \cdot \boldsymbol{\sigma}_j - E_{10} \mathbf{k}_i \cdot \boldsymbol{\sigma}_i \mathbf{k}_j \cdot \boldsymbol{\sigma}_j \boldsymbol{\tau}_i \cdot \boldsymbol{\tau}_j \\
& - E_{11} \mathbf{k}_i \cdot \boldsymbol{\sigma}_j \mathbf{k}_j \cdot \boldsymbol{\sigma}_i - E_{12} \mathbf{k}_i \cdot \boldsymbol{\sigma}_j \mathbf{k}_j \cdot \boldsymbol{\sigma}_i \boldsymbol{\tau}_i \cdot \boldsymbol{\tau}_j \\
& \left. - E_{13} \mathbf{k}_i \cdot \boldsymbol{\sigma}_j \mathbf{k}_j \cdot \boldsymbol{\sigma}_i \boldsymbol{\tau}_i \cdot \boldsymbol{\tau}_k \right) \\
& \equiv \sum_{i=1}^{13} E_i O_i, \tag{37}
\end{aligned}$$

where $\mathbf{k}_i = \mathbf{p}'_i - \mathbf{p}_i$, $\mathbf{Q}_i = \frac{\mathbf{p}_i + \mathbf{p}'_i}{2}$. Specifically, we have

$$U^\dagger V_{NN}^{(0)} U = \sum_{i=1}^{13} \delta E_i O_i, \tag{38}$$

with ¹

$$\delta E_1 = \alpha_1 (C_S + C_T) + \alpha_2 (C_S - 2C_T), \tag{39}$$

$$\delta E_2 = 3\alpha_2 C_T + 2\alpha_3 C_T - 8\alpha_4 C_T + 2\alpha_5 C_T, \tag{40}$$

$$\begin{aligned}
\delta E_3 = & 2\alpha_1 C_T + \alpha_2 (2C_S - C_T) + \frac{2}{3} \alpha_3 (2C_S - C_T) \\
& + 8\alpha_4 C_T - 2\alpha_5 C_T, \tag{41}
\end{aligned}$$

$$\begin{aligned}
\delta E_4 = & \frac{2}{3} \alpha_1 C_T + \frac{1}{3} \alpha_2 (2C_S - 7C_T) - \frac{2}{3} \alpha_3 C_T \\
& + \frac{8}{3} \alpha_4 C_T - \frac{2}{3} \alpha_5 C_T, \tag{42}
\end{aligned}$$

$$\begin{aligned}
\delta E_5 = & 2\alpha_1 C_T + 2\alpha_2 (C_S - 2C_T) + \frac{2}{3} \alpha_3 (2C_S - C_T) \\
& + 8\alpha_4 C_T - 2\alpha_5 C_T, \tag{43}
\end{aligned}$$

$$\begin{aligned}
\delta E_6 = & \frac{2}{3} \alpha_1 C_T + \frac{2}{3} \alpha_2 (C_S - 2C_T) - \frac{2}{3} \alpha_3 C_T + \frac{8}{3} \alpha_4 C_T \\
& - \frac{2}{3} \alpha_5 C_T, \tag{44}
\end{aligned}$$

$$\delta E_7 = 24\alpha_4 C_T, \tag{45}$$

$$\delta E_8 = \frac{1}{3} \delta E_7, \tag{46}$$

$$\begin{aligned}
\delta E_9 = & 3\alpha_1 C_T + 3\alpha_2 (C_S - 2C_T) + 2\alpha_3 (C_S - 2C_T) \\
& - \alpha_4 (C_S - 11C_T) + 2\alpha_5 (C_S - 2C_T), \tag{47}
\end{aligned}$$

$$\begin{aligned}
\delta E_{10} = & \alpha_1 C_T + \alpha_2 (C_S - 2C_T) - \frac{1}{3} \alpha_4 (3C_S - 15C_T), \\
& \tag{48}
\end{aligned}$$

¹ We correct here some wrong factors in Ref. [13].

$$\delta E_{11} = 3\alpha_1 C_T + 3\alpha_2 (C_S - 2C_T) + 2\alpha_3 (C_S - 2C_T) + \alpha_4 (C_S - 11C_T) - 2\alpha_5 (C_S - 2C_T), \quad (49)$$

$$\delta E_{12} = \alpha_1 C_T + \alpha_2 (C_S - 2C_T) + \frac{1}{3}\alpha_4 (3C_S - 15C_T), \quad (50)$$

$$\delta E_{13} = -16\alpha_4 C_T + 4\alpha_5 C_T. \quad (51)$$

With the specific choice for the unitary transformation encoded in Eqs. (18)-(22), the 3N contact LECs E_i in Eq. (37) are shifted to

$$E_i \rightarrow \tilde{E}_i = E_i + \delta E_i, \quad (52)$$

where the induced contributions δE_i are enhanced as compared to the genuine ones E_i , due to the presence of the nucleon mass factor, scaling as $m \sim O(\Lambda_\chi^2/p)$ in the Weinberg counting [27], which effectively promotes them to N3LO. From now on, the LECs E_i will be thought of as constituted only of the induced contributions, $E_i = \delta E_i$. Thus, at N3LO the 3N contact interaction depends on five combinations of the 2N LECs D_i , appearing in Eqs. (18)-(22), which cannot be determined from 2N scattering data, but have to be fitted to experimental observables in $A > 2$ systems.

In the following we explore the sensitivity of polarization observables in low-energy $N - d$ scattering to these five combinations of LECs. Since we take the phenomenological AV18 as representative of a realistic 2N interaction, we should clarify the meaning of the LECs C_S and C_T in this framework. As a reasonable estimate, based on studies of universal behavior [14], we take them from a fit of the LO 2N contact interaction (36)

$$V_{NN,\Lambda}^{(0)} = [C_S + C_T \boldsymbol{\sigma}_1 \cdot \boldsymbol{\sigma}_2] Z_\Lambda(r) \quad (53)$$

to the singlets and triplets $n - p$ scattering lengths as predicted by the AV18 potential. In other words, we treat the contact potential (53) as a very low-energy representation of the AV18 potential. In the above expression a local cutoff has been introduced,

$$Z_\Lambda(r) = \int \frac{d\mathbf{p}}{(2\pi)^3} e^{i\mathbf{p}\cdot\mathbf{r}} F(\mathbf{p}^2; \Lambda), \quad (54)$$

with

$$F(\mathbf{p}^2, \Lambda) = \exp \left[- \left(\frac{\mathbf{p}^2}{\Lambda^2} \right)^2 \right], \quad (55)$$

and $\Lambda = 500$ MeV. From this procedure we get

$$C_S = -66.53 \text{ GeV}^{-2}, \quad C_T = -3.47 \text{ GeV}^{-2}. \quad (56)$$

The same cutoff is also used in the coordinate space expression of the induced 3N contact interaction, which be-

comes

$$\begin{aligned} V_{3N,\Lambda}^{(2)} = & \sum_{ijk} [E_1 + E_2 \boldsymbol{\tau}_i \cdot \boldsymbol{\tau}_j + (E_3 + E_4 \boldsymbol{\tau}_i \cdot \boldsymbol{\tau}_j) \boldsymbol{\sigma}_i \cdot \boldsymbol{\sigma}_j] \\ & \times \left[Z_\Lambda''(r_{ij}) + 2 \frac{Z_\Lambda'(r_{ij})}{r_{ij}} \right] Z_\Lambda(r_{ik}) \\ & + (E_5 + E_6 \boldsymbol{\tau}_i \cdot \boldsymbol{\tau}_j) S_{ij} \left[Z_\Lambda''(r_{ij}) - \frac{Z_\Lambda'(r_{ij})}{r_{ij}} \right] Z_\Lambda(r_{ik}) \\ & + (E_7 + E_8 \boldsymbol{\tau}_i \cdot \boldsymbol{\tau}_k) (\mathbf{L} \cdot \mathbf{S})_{ij} \frac{Z_\Lambda'(r_{ij})}{r_{ij}} Z_\Lambda(r_{ik}) \\ & + [(E_9 + E_{10} \boldsymbol{\tau}_j \cdot \boldsymbol{\tau}_k) \boldsymbol{\sigma}_j \cdot \hat{\mathbf{r}}_{ij} \boldsymbol{\sigma}_k \cdot \hat{\mathbf{r}}_{ik} \\ & + (E_{11} + E_{12} \boldsymbol{\tau}_j \cdot \boldsymbol{\tau}_k + E_{13} \boldsymbol{\tau}_i \cdot \boldsymbol{\tau}_j) \boldsymbol{\sigma}_k \cdot \hat{\mathbf{r}}_{ij} \boldsymbol{\sigma}_j \cdot \hat{\mathbf{r}}_{ik}] \\ & \times Z_\Lambda'(r_{ij}) Z_\Lambda'(r_{ik}), \end{aligned} \quad (57)$$

where S_{ij} and $(\mathbf{L} \cdot \mathbf{S})_{ij}$ are respectively the tensor and spin-orbit operators for particles i and j .

IV. LOW-ENERGY P-D SCATTERING OBSERVABLES WITHIN THE HH METHOD

In order to solve the 3-body Schrödinger equation we used the HH method, (see Refs. [22, 23] for reviews). Below the deuteron breakup threshold, the $N - d$ scattering wave function is expressed as the sum of an internal and an asymptotic part as

$$\Psi_{LSJJ_z} = \Psi_C + \Psi_A, \quad (58)$$

where the internal part Ψ_C is expanded in HH as

$$\Psi_C = \sum_{\mu} c_{\mu} \Phi_{\mu}. \quad (59)$$

Here μ denotes all the quantum numbers required to fully define the basis element. The asymptotic part, Ψ_A , describes the relative motion between the nucleon and the deuteron at large distance. This latter is a linear combination of the regular and irregular solutions of the free (or Coulomb) $N - d$ Schrödinger equation, properly regularized at small distances [15]. Denoting these solutions with $\Omega_{LSJJ_z}^{\lambda}$, $\lambda = R, I$ respectively, and defining

$$\Omega_{LSJJ_z}^{\pm} = i\Omega_{LSJJ_z}^R \pm \Omega_{LSJJ_z}^I, \quad (60)$$

we have

$$\Psi_A = \Omega_{LSJJ_z}^- + \sum_{L'S'} \mathcal{S}_{LS,L'S'}^J(q) \Omega_{L'S'JJ_z}^+. \quad (61)$$

Here $\mathcal{S}_{LS,L'S'}^J$ are the S -matrix elements and q is defined as the modulus of the $N - d$ relative momentum. From the S -matrix it is possible to compute phase shift and mixing angles, from which the scattering observables are obtained. The S -matrix in Eq. (61) and the coefficients c_{μ} in Eq. (59) are obtained from the complex formulation

of the Kohn variational principle² [28]. This principle requires that the functional

$$[\mathcal{S}_{LS,L'S'}^J(q)] = \mathcal{S}_{LS,L'S'}^J(q) - \frac{i}{2} \langle \Psi_{LSJJ_z} | H - E | \Psi_{L'S'JJ_z} \rangle \quad (62)$$

be stationary under variations of the trial parameters in Ψ_{LSJJ_z} , with the asymptotic part normalized as

$$\langle \Omega_{LSJJ_z}^R | H - E | \Omega_{LSJJ_z}^I \rangle - \langle \Omega_{LSJJ_z}^I | H - E | \Omega_{LSJJ_z}^R \rangle = 1. \quad (63)$$

This implies that the weights $\mathcal{S}_{LS,L'S'}^J$ must solve the linear system

$$\sum_{\tilde{L}\tilde{S}} \mathcal{S}_{LS,\tilde{L}\tilde{S}}^J X_{L'S',\tilde{L}\tilde{S}} = Y_{LS,L'S'} \quad (64)$$

with

$$X_{LS,L'S'} = \langle \Omega_{LSJJ_z}^+ | H - E | \Psi_C^+ + \Omega_{L'S'JJ_z}^+ \rangle, \quad (65)$$

$$Y_{LS,L'S'} = \langle \Omega_{LSJJ_z}^- + \Psi_C^- | E - H | \Omega_{L'S'JJ_z}^+ \rangle. \quad (66)$$

Here the functions Ψ_C^\pm are given in Eq. (59) with the coefficients c_μ^\pm being the solutions of

$$\sum_{\mu'} \langle \Phi_\mu | H - E | \Phi_{\mu'} \rangle c_{\mu'}^\pm = - \langle \Phi_\mu | H - E | \Omega_{LSJJ_z}^\pm \rangle. \quad (67)$$

Substituting the calculated weights $\mathcal{S}_{LS,L'S'}^J$ of Eq. (64) into Eq. (62), it is possible to obtain a second order estimate. In order to solve the linear system of Eq. (64), the matrix elements of the Hamiltonian H in Eqs. (65), (66) and (67) have to be computed between the HH basis elements and the asymptotic functions. We decompose the Hamiltonian as

$$H = H_{NN} + V_{3N,\Lambda}^{(0)} + V_{3N,\Lambda}^{(2)}, \quad (68)$$

where H_{NN} is the Hamiltonian containing the kinetic energy T plus the AV18 2N interaction with Coulomb potential and $V_{3N,\Lambda}^{(0)} + V_{3N,\Lambda}^{(2)}$ contain the 3N interaction. Specifically, we consider, in addition to the induced contact interaction (57), a leading order contact interaction,

$$V_{3N,\Lambda}^{(0)} = E_0 \sum_{ijk} Z_\Lambda(r_{ij}) Z_\Lambda(r_{ik}). \quad (69)$$

Written $V_{3N,\Lambda}^{(0)} = E_0 V_0$ and $V_{3N,\Lambda}^{(2)} = \sum_{i=1,13} E_i V_i$, the linear system of Eq. (67) results

$$\sum_{\mu'} c_{\mu'}^\lambda \left\langle \Phi_\mu \left| H_{NN} + \sum_{i=0,13} E_i V_i - E \right| \Phi_{\mu'} \right\rangle = - \left\langle \Phi_\mu \left| H_{NN} + \sum_{i=0,13} E_i V_i - E \right| \Omega_{LSJJ_z}^\lambda \right\rangle, \quad (70)$$

which can be put in the matrix form

$$\sum_{\mu'} \left[(H_{NN})_{\mu\mu'} + \sum_{i=0,13} E_i (V_i)_{\mu\mu'} - E N_{\mu\mu'} \right] c_{\mu'}^\lambda = - (H_{NN})_{\mu\lambda} + \sum_{i=0,13} E_i (V_i)_{\mu\lambda} - E N_{\mu\lambda}. \quad (71)$$

Here $()_{\mu\mu'}$ denotes the matrix elements of the considered operator between the corresponding basis states. The contact potential matrix can be computed as a linear combination of several matrices, one for $V^{(0)}$ and one for each operator appearing in $V^{(2)}$. With the proper corresponding LECs, these matrices can be constructed once and used for all purposes. Their size is approximately 2000×2000 , making the computation feasible in few seconds for each channel on an ordinary desktop. With these dimensions the observables are calculated well inside a 1% accuracy [30–32]. A specific set of LECs can be utilized to compute the associated S -matrix for each J^π state using the Kohn variational principle, from which the observables at a specific energy E can be obtained. In order to do this, we compute the $N - d$ transition matrix M , which is composed of the Coulomb amplitude $f_c(\theta_{\text{cm}})$ and a nuclear term, θ_{cm} being the center-of-mass scattering angle, as

$$M_{\nu\nu'}^{SS'}(\theta_{\text{cm}}) = f_c(\theta_{\text{cm}}) \delta_{SS'} \delta_{\nu\nu'} + \frac{\sqrt{4\pi}}{q} \sum_{LL'J} \sqrt{2L+1} (L0, S\nu | J\nu) (L'M', S'\nu' | J\nu) e^{i(\sigma_L + \sigma_{L'} - 2\sigma_0)} T_{LS,L'S'}^J Y_{L'M'}(\theta_{\text{cm}}, 0). \quad (72)$$

Here the matrix $M_{\nu\nu'}^{SS'}(\theta_{\text{cm}})$ is a 6×6 matrix corresponding to the couplings of the spin 1 of the deuteron and the spin 1/2 of the third nucleon, to $S, S' = 1/2$ or $3/2$ with projections ν, ν' . The quantum numbers L, L' are the relative orbital angular momentum between the deuteron and the third particle and J is the total angular momentum. The matrix elements $T_{LS,L'S'}^J$ form the T -matrix of a Hamiltonian containing the nuclear plus Coulomb interactions. Note that the T -matrix can be related with the S -matrix of Eq. (61) by $S = 1 - 2i\pi T$. Finally, σ_L are the Coulomb phase-shifts. The effect of other components of the electromagnetic interaction are discussed in Ref. [33].

V. FIT RESULTS

The observables used in the fitting procedure are the $p - d$ differential cross section, the two vector analyzing powers A_y and iT_{11} , the three tensor analyzing powers T_{20}, T_{21}, T_{22} and the doublet and quartet $n - d$ scattering lengths. In particular we determine the leading contact LEC E_0 from the experimental triton binding energy. Then, we fit the experimental doublet and quartet $n - d$

² We remind that all the states appearing in the bras $\langle \Psi |$ should be understood as $\langle \tilde{\Psi} |$ where $\tilde{\Psi}$ is the complex conjugate of Ψ [29].

scattering lengths [34, 35] and the six $p-d$ scattering observables at center-of-mass energy $E_{\text{cm}} = 2$ MeV [24], amounting to 282 experimental data. The theoretical observables are calculated solving Eqs. (64) and (67), then the obtained S -matrix is used to calculate the transition matrix M of Eq. (72), from which the observables are directly calculated [36]. At the energy considered, states up to $L = 2$ are calculated using the full Hamiltonian, whereas for $L > 2$ the three-body potential was neglected due to its short-range character (see also Ref. [37]), while the strong two-body potential was included up to a maximum value of $L = 6$ in the partial wave expansion of the observables, which is enough at the energy of interest.

For the differential cross section we include in the χ^2 definition an overall normalization factor Z of the data points, i.e

$$\chi^2 = \sum_i \frac{(d_i^{\text{exp}}/Z - d_i^{\text{th}})^2}{(\sigma_i^{\text{exp}}/Z)^2}, \quad (73)$$

with Z obtained from the minimization condition as

$$Z = \frac{\sum_i d_i^{\text{exp}} d_i^{\text{th}} / (\sigma_i^{\text{exp}})^2}{\sum_i (d_i^{\text{th}})^2 / (\sigma_i^{\text{exp}})^2}. \quad (74)$$

In Eqs. (73) and (74) $d_i^{\text{exp}/\text{th}}$ are the experimental data points and their theoretical predictions, while σ_i^{exp} is the experimental error. In our study we have checked that Z never differs from 1 by more than 2% [38]. For the other observables, we treat the normalization $Z = 1.00 \pm 0.01$ as an additional experimental datum since, according to Ref. [24], the systematic uncertainty is estimated as 1%.

For an initial random set of the five α_i parameters of Eqs. (18)-(22), we solve the scattering problem and calculate the corresponding observables. Using the POUNDERs algorithm [39] we start an iterative procedure to minimize the global $\chi^2/\text{d.o.f.}$ of the data set description. Using different initial random input of α_i values, we repeat the algorithm trying to localize the deepest minimum. This amounts to $\chi^2/\text{d.o.f.} = 1.7$, of the same quality as the most accurate multiparameter fits to the same data performed so far [19].

Fig. 1 shows the best fit curve for the A_y and iT_{11} analyzing power in $\vec{p}-d$ and $\vec{d}-p$ scattering, compared to the predictions from the purely 2N AV18 interaction and from the addition of the Urbana IX 3N interaction. We conclude that the effective N3LO induced 3N contact interaction allows to solve the long-standing A_y problem. Also the description of the vector analyzing power iT_{11} is drastically improved.

We also show in the same figure the best fit curve obtained from a 3-parameter fit which does not include the α -parameters of the \mathbf{P} -dependent N3LO 2N contact interaction, i.e. with $\alpha_4 = \alpha_5 = 0$, in order to assess the relevance of the LECs D_{16} and D_{17} , which were never considered before. No spin-orbit operators, of the kind

Fitting procedure	5-param.	3-param.
$\chi^2/\text{d.o.f.}$	1.7	2.3
e_0	0.685	-1.570
$\tilde{\alpha}_1 C_S$	1.410	-3.611
$\tilde{\alpha}_2 C_S$	0.211	-0.483
$\tilde{\alpha}_3 C_S$	-0.370	0.209
$\tilde{\alpha}_4 C_S$	1.735	0
$\tilde{\alpha}_5 C_S$	2.266	0
${}^2a_{nd}$ [fm]	6.31	6.32
${}^4a_{nd}$ [fm]	0.648	0.647

TABLE I. Results of the 5-parameters and 3-parameters fits, the latter one obtained ignoring the \mathbf{P} -dependent 2N contact interaction, i.e. setting $\alpha_4 = \alpha_5 = 0$. See text for more explanations.

proposed in Ref. [40], are present in this latter case, and the minimum $\chi^2/\text{d.o.f.}$ increases to 2.3.

In Fig. 2 we show the same curves for the tensor analyzing powers of $\vec{d}-p$ elastic scattering and for the differential cross-section. By inspection of the figures, we can conclude that all the observables are nicely reproduced.

The fitted parameters α_i are displayed in Table I, together with the corresponding values of the LO 3N contact LEC E_0 in units as dictated by naive dimensional analysis [41, 42], i.e.

$$e_0 = E_0 F_\pi^4 \Lambda, \quad \tilde{\alpha}_i = \alpha_i F_\pi^4 \Lambda^3, \quad (75)$$

where $F_\pi = 92.4$ MeV is the pion decay constant. Also shown in the table are the doublet and quartet $n-d$ scattering lengths, to be compared with the experimental values ${}^2a_{nd} = (0.645 \pm 0.003 \pm 0.007)$ fm [34] and ${}^4a_{nd} = (6.35 \pm 0.02)$ fm [35]. It is interesting to observe that the fitted 3N interaction parameters are of a natural size for a N3LO contribution. In order to see this, we can translate the values of the α_i 's into combinations of the N3LO 2N LECs D_i 's using Eqs. (18)-(22). This is done in Table II for the two fitting procedures. As a reference, we report in the same table the corresponding combinations of LECs obtained from 2N data in Ref. [4], and used in the Idaho N3LO 2N chiral potential with $\Lambda = 500$ MeV. The comparison of the actual values has little meaning, also due to the hybrid character of our calculation. However it is interesting to observe that the orders of magnitude are the same. In particular, for the 5-parameter fit, the LECs combinations are not larger than those obtained in the Idaho N3LO chiral potential. We advocate that, were those combinations fitted in the $A = 3$ system, the A_y puzzle would be solved at N3LO. However this remains to be seen explicitly in a consistent chiral calculation.

VI. CONCLUSIONS

A suitable choice of unitary transformation allows to reduce the number of LECs parametrizing the N3LO 2N contact interaction to twelve. This procedure generates a

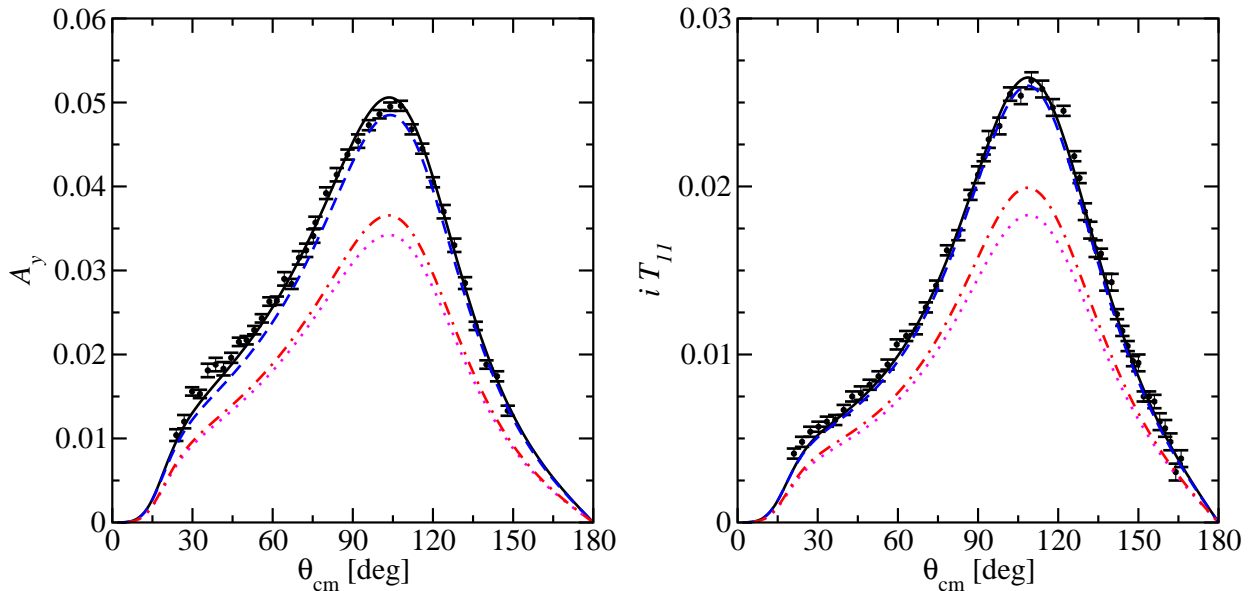


FIG. 1. Proton and deuteron analyzing power in $\vec{p}-d$ and $\vec{d}-p$ scattering at $E_{\text{cm}} = 2$ MeV. The full (black) lines result from a global 5-parameter fit, the dashed (blue) lines from a 3-parameter fit excluding the \mathbf{P} -dependent 2N interaction, the dotted (pink) lines are the predictions from the 2N AV18 potential, while the dashed-dotted (red) lines are the predictions including also the 3N Urbana IX interaction. Experimental data are from Ref. [24].

	5-param.	3-param.	Ref.[4]
D_{16}	-0.610	0	-
D_{17}	-0.536	-0.181	-
$16D_1 + D_2 + 4D_3$	-3.96	10.86	6.41
$16D_5 + D_6 + 4D_7$	-0.593	1.21	4.05
$D_{14} + 16D_{11} + 4D_{12} + 4D_{13}$	2.08	-1.44	-3.04

TABLE II. Estimation of some N3LO LECs combinations, the D_i are in units of 10^4 GeV^{-4} . In the second column we show the values obtained from the 5-parameter fit, in the third one the estimates obtained from the 3-parameter fit, while the last column shows the values obtained in Ref. [4] and used for the Idaho N3LO 2N potential with $\Lambda = 500$ MeV.

3N interaction depending on five unconstrained LECs. In the present paper we examined the effect of this induced 3N interaction on polarization observables of $p-d$ scattering below the breakup threshold. We showed that the LECs can be adjusted allowing to solve the long-standing A_y puzzle.

The induced 3N interaction can be thought of as a specific off-shell extension of the 2N interaction, leaving the 2N observables unchanged. Such off-shell extension of the 2N potentials were considered in the past (see e.g. Ref. [43]) and found to have a prominent role in the $N-d$ A_y puzzle [44]. We remark in passing that a satisfactory fit (with $\chi^2/\text{d.o.f.} = 1.8$) can be obtained even without including any 3N interaction except for the induced one, i.e. with $E_0 = 0$. We emphasize that the novelty of our proposal lies in the identification of its precise form in the context of a systematic low-energy expansion, where

it starts to contribute at N3LO. This statement has also a quantitative content, despite all the limitations of our hybrid calculation, in light of the comparison of the magnitudes of the involved LECs with those inferred within the ChEFT framework of the 2N interaction, as shown in Table II.

Of course it will be interesting to repeat the above analysis in a fully consistent ChEFT framework for 2N and 3N interactions. In this respect, also the induced 3N interaction from the unitary transformation of the one-pion exchange 2N potential has to be taken into account. To the best of our knowledge such contribution, first worked out in Ref. [13], has never been considered in the literature so far. In the present work it was implicitly taken into account through the values of the LECs C_S and C_T , by considering a pionless representation of the AV18 potential. It will be also necessary to explore the energy dependence of the predicted $p-d$ scattering observables and confront it with experimental data. Such exploration has been pursued in Ref. [19] to energies lower than $E_{\text{cm}} = 2$ MeV using a restricted form for the subleading 3N contact interaction, leading to quite satisfactory results. Finally, the same shuffling of contact operators between the 2N and 3N sectors applies to the pionless formulation of the EFT. The counting of the induced 3N operators examined in the present paper should follow from the corresponding counting of the 2N operators. A further peculiarity in this case is the promotion of the 3N force to LO. Thus the appropriate counting should be re-examined in this perspective (see also Ref. [45]). Work along the lines outlined above is deferred to forthcoming investigations.

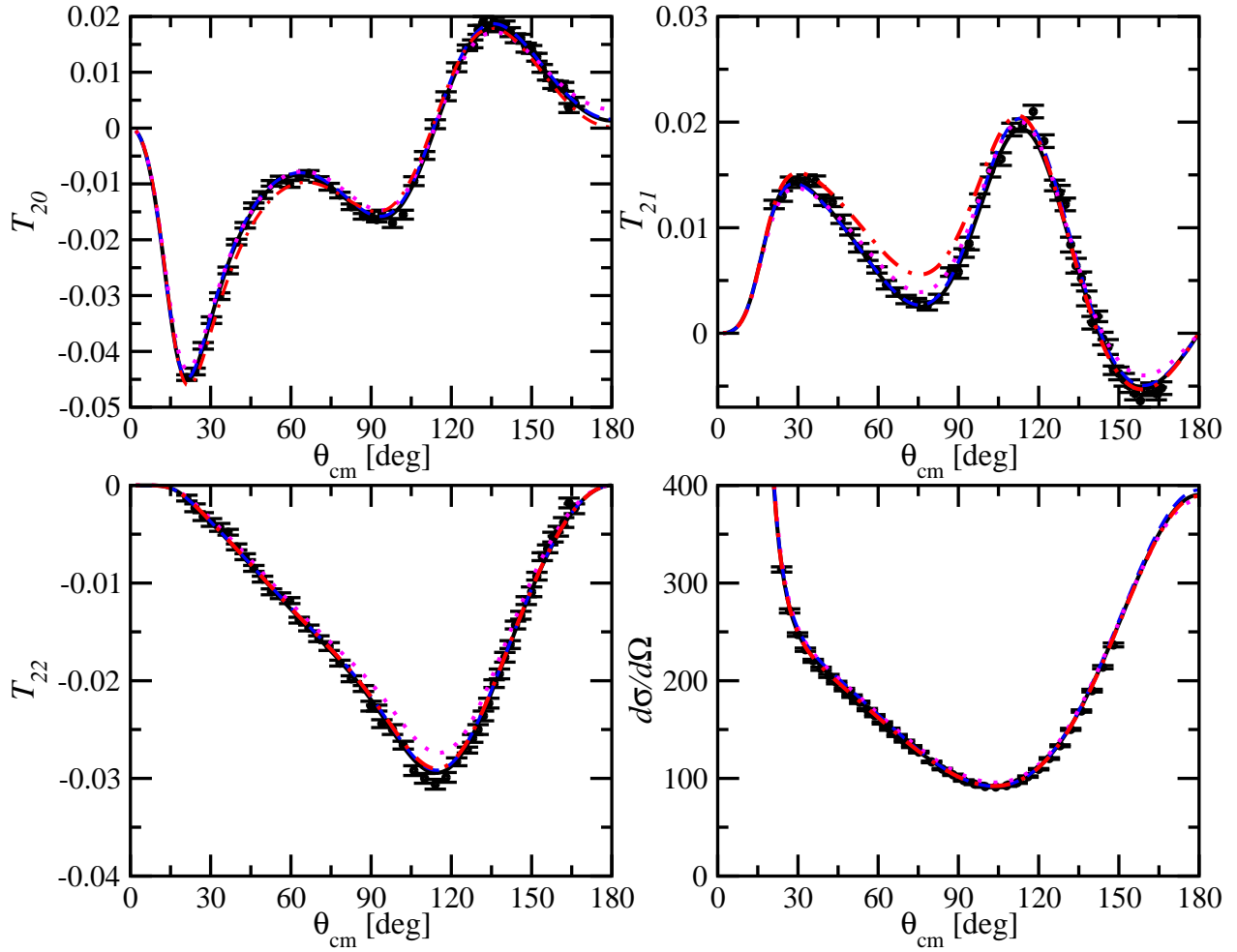


FIG. 2. Same as Fig. 1 but for T_{20} , T_{21} , T_{22} tensor observables in $\vec{d}-p$ scattering and for the unpolarized differential cross-section at $E_{\text{cm}} = 2$ MeV.

-
- [1] P. F. Bedaque and U. van Kolck, *Ann. Rev. Nucl. Part. Sci.* **52**, 339-396 (2002).
- [2] E. Epelbaum, *Prog. Part. Nucl. Phys.* **57**, 654-741 (2006).
- [3] E. Epelbaum, H. W. Hammer and U. G. Meissner, *Rev. Mod. Phys.* **81**, 1773-1825 (2009).
- [4] R. Machleidt and D. R. Entem, *Phys. Rept.* **503**, 1-75 (2011).
- [5] E. Epelbaum, A. Nogga, W. Gloeckle, H. Kamada, U. G. Meissner and H. Witala, *Phys. Rev. C* **66**, 064001 (2002).
- [6] P. Navratil, *Few Body Syst.* **41**, 117-140 (2007).
- [7] A. Gardestig and D. R. Phillips, *Phys. Rev. Lett.* **96**, 232301 (2006).
- [8] D. Gazit, S. Quaglioni and P. Navratil, *Phys. Rev. Lett.* **103**, 102502 (2009) [erratum: *Phys. Rev. Lett.* **122**, no.2, 029901 (2019)].
- [9] L. E. Marcucci, A. Kievsky, S. Rosati, R. Schiavilla and M. Viviani, *Phys. Rev. Lett.* **108**, 052502 (2012) [erratum: *Phys. Rev. Lett.* **121**, no.4, 049901 (2018)].
- [10] L. Ceccarelli, A. Gnech, L. E. Marcucci, M. Piarulli and M. Viviani, *Front. Phys.* **10**, 1049919 (2023).
- [11] L. Girlanda, A. Kievsky and M. Viviani, *Phys. Rev. C* **84**, no.1, 014001 (2011) [erratum: *Phys. Rev. C* **102**, no.1, 019903 (2020)].
- [12] P. Reinert, H. Krebs and E. Epelbaum, *Eur. Phys. J. A* **54**, no.5, 86 (2018).
- [13] L. Girlanda, A. Kievsky, L. E. Marcucci and M. Viviani, *Phys. Rev. C* **102**, 064003 (2020).
- [14] A. Kievsky, M. Gattobigio, L. Girlanda and M. Viviani, *Ann. Rev. Nucl. Part. Sc.* **71** (2021).
- [15] M. Abramowitz and I. Stegun, Dover, New York, ninth Dover printing, tenth GPO printing edition, (1964)
- [16] V. Bernard, E. Epelbaum, H. Krebs and U. G. Meissner, *Phys. Rev. C* **77**, 064004 (2008).
- [17] V. Bernard, E. Epelbaum, H. Krebs and U. G. Meissner, *Phys. Rev. C* **84**, 054001 (2011).
- [18] J. Golak, R. Skibinski, K. Topolnicki, H. Witala, E. Epelbaum, H. Krebs, H. Kamada, U. G. Meissner, V. Bernard and P. Maris, *et al.* *Eur. Phys. J. A* **50**, 177 (2014).
- [19] L. Girlanda, A. Kievsky, M. Viviani and L. E. Marcucci,

- Phys. Rev. C **99**, no.5, 054003 (2019).
- [20] H. Witała, J. Golak and R. Skibiński, Phys. Rev. C **105**, no.5, 054004 (2022).
- [21] R. B. Wiringa, V. G. J. Stoks and R. Schiavilla, Phys. Rev. C **51**, 38-51 (1995).
- [22] A. Kievsky, S. Rosati, M. Viviani, L. E. Marcucci and L. Girlanda, J. Phys. G **35**, 063101 (2008).
- [23] L. E. Marcucci, J. Dohet-Eraly, L. Girlanda, A. Gnech, A. Kievsky and M. Viviani, Front. in Phys. **8**, 69 (2020).
- [24] S. Shimizu, K. Sagara, H. Nakamura, K. Maeda, T. Miwa, N. Nishimori, S. Ueno, T. Nakashima and S. Morinobu, Phys. Rev. C **52**, 1193-1202 (1995).
- [25] D. R. Entem and R. Machleidt, Phys. Lett. B **524**, 93-98 (2002).
- [26] D. R. Entem and R. Machleidt, Phys. Rev. C **68**, 041001 (2003).
- [27] S. Weinberg, Nucl. Phys. B **363**, 3-18 (1991).
- [28] A. Kievsky, Nucl. Phys. A **624**, 125-139 (1997).
- [29] R. R. Lucchese, Phys. Rev. A **40**, 6879-6885 (1989).
- [30] A. Nogga, A. Kievsky, H. Kamada, W. Gloeckle, L. E. Marcucci, S. Rosati and M. Viviani, Phys. Rev. C **67**, 034004 (2003).
- [31] A. Kievsky, J. L. Friar, G. L. Payne, S. Rosati and M. Viviani, Phys. Rev. C **63**, 064004 (2001).
- [32] A. Kievsky, M. Viviani, S. Rosati, D. Huber, W. Gloeckle, H. Kamada, H. Witala and J. Golak, Phys. Rev. C **58**, 3085-3092 (1998).
- [33] A. Kievsky, M. Viviani and L. E. Marcucci, Phys. Rev. C **69**, 014002 (2004).
- [34] W. Dilg, L. Koester and W. Nistler, Phys. Lett. B **36**, 208-210 (1971).
- [35] K. Schoen, D. L. Jacobson, M. Arif, P. R. Huffman, T. C. Black, W. M. Snow, S. K. Lamoreaux, H. Kaiser and S. A. Werner, Phys. Rev. C **67**, 044005 (2003).
- [36] W. Gloeckle, H. Witala, D. Huber, H. Kamada and J. Golak, Phys. Rept. **274**, 107-285 (1996).
- [37] A. Kievsky, S. Rosati, W. Tornow and M. Viviani, Nucl. Phys. A **607**, 402-424 (1996).
- [38] A. Kievsky, M. Viviani and S. Rosati, Phys. Rev. C **64**, 024002 (2001).
- [39] T. Munson, J. Sarich, S. Wild, S. Benson and L. McInnes, TAO 2.0 Users Manual, Technical Report ANL/MCS-TM-322, <http://www.mcs.anl.gov/tao>
- [40] A. Kievsky, Phys. Rev. C **60**, 034001 (1999).
- [41] A. Manohar and H. Georgi, Nucl. Phys. B **234**, 189-212 (1984).
- [42] H. Georgi, Phys. Lett. B **298**, 187-189 (1993).
- [43] P. Doleschall and I. Borbely, Phys. Rev. C **62**, 054004 (2000).
- [44] P. Doleschall, Phys. Rev. C **69**, 054001 (2004).
- [45] A. Kievsky, M. Viviani, M. Gattobigio and L. Girlanda, Phys. Rev. C **95**, no.2, 024001 (2017).